



Minerva Access is the Institutional Repository of The University of Melbourne

Author/s:

Steinschneider, S;Ho, M;Williams, AP;Cook, ER;Lall, U

Title:

A 500-Year Tree Ring-Based Reconstruction of Extreme Cold-Season Precipitation and Number of Atmospheric River Landfalls Across the Southwestern United States

Date:

2018-06-16

Citation:

Steinschneider, S., Ho, M., Williams, A. P., Cook, E. R. & Lall, U. (2018). A 500-Year Tree Ring-Based Reconstruction of Extreme Cold-Season Precipitation and Number of Atmospheric River Landfalls Across the Southwestern United States. *Geophysical Research Letters*, 45 (11), pp.5672-5680. <https://doi.org/10.1029/2018GL078089>.

Persistent Link:

<https://hdl.handle.net/11343/285198>

Steinschneider Scott (Orcid ID: 0000-0002-8882-1908)
Ho Michelle (Orcid ID: 0000-0002-1513-8016)
Williams A., Park (Orcid ID: 0000-0001-8176-8166)
Cook Edward, R (Orcid ID: 0000-0001-7478-4176)
Lall Upmanu (Orcid ID: 0000-0003-0529-8128)

**A 500-year tree-ring based reconstruction of extreme cold-season precipitation and number
of atmospheric river landfalls across the Southwestern U.S.**

Scott Steinschneider¹, Michelle Ho², A. Park Williams³, Edward R. Cook⁴, Upmanu Lall⁵

1. Assistant Professor, Department of Biological and Environmental Engineering, Cornell University, Ithaca, NY, 14853. Email: ss3378@cornell.edu, Phone: 607-255-2155 (Corresponding Author)
2. Associate Research Scientist, Department of Earth & Environmental Engineering, Columbia University, New York, NY, 10027. Email: mh3538@columbia.edu, Phone: 212-854-7081
3. Associate Research Scientist, Tree Ring Lab, Lamont-Doherty Earth Observatory, Palisades, NY, 10964. Email: williams@ldeo.columbia.edu, Phone: 845-365-8193
4. Ewing Lamont Research Professor, Tree Ring Lab, Lamont-Doherty Earth Observatory, Palisades, NY, 10964. Email: drdendro@ldeo.columbia.edu, Phone: 845-365-8618
5. Professor, Department of Earth & Environmental Engineering, Columbia University, NYC, NY, 10027. Email: ula2@columbia.edu, Phone: 212-854-7081

Key Points

#1: The first two EOFs of a reconstructed drought index in the Southwest US relate to two major atmospheric river storm tracks over the region.

This is the author manuscript accepted for publication and has undergone full peer review but has not been through the copyediting, typesetting, pagination and proofreading process, which may lead to differences between this version and the [Version of Record](#). Please cite this article as doi: [10.1029/2018GL078089](https://doi.org/10.1029/2018GL078089)

#2: A network of tree-ring chronologies in the Southwest can accurately reconstruct landfalling atmospheric rivers along the southwest coast.

#3: The network of chronologies can also reconstruct the occurrence of extreme precipitation along the southern California coastline.

Keywords: atmospheric river; tree-ring chronologies; reconstruction; extreme precipitation

Abstract

This study develops a reconstruction of the frequency of extreme cold-season precipitation and the occurrence of landfalling atmospheric river (AR) storm tracks across the Southwestern U.S. using a network of tree-ring chronologies and the Living Blended Drought Atlas (LBDA), a 500-year tree-ring based reconstruction of the summer Palmer Drought Severity Index. The first two rotated EOFs of the LBDA across the Southwest are shown to relate well to previously identified patterns of regional AR activity. Accordingly, the rotated EOFs also record patterns of extreme precipitation associated with those ARs, albeit with some uncertainty introduced by non-extreme precipitation. A network of chronologies sensitive to cold-season precipitation is then used to reconstruct the occurrence of landfalling ARs and extreme precipitation along the southern Californian coast, demonstrating for the first time the feasibility of reconstructing AR landfalls and extreme events in the Southwest based on spatial patterns in a network of dendroclimatic proxies.

Plain Language Summary

Extreme precipitation and flood events are a significant hazard to society. Along the U.S. west coast, many of these extreme events are linked to a particular type of storm called an atmospheric river. Intense atmospheric rivers that make landfall are rare, and this makes it difficult to assess the likelihood of these storms and whether this likelihood is changing over time. In this study, we present the first attempt to predict the occurrence of landfalling atmospheric rivers impacting the southwest coast of the U.S. over the past 500 years, as well as extreme precipitation associated with these storms. To do this, we use a series of tree-ring chronologies that record winter precipitation amounts in the widths of tree rings, which for some trees can extend backward in time for hundreds of years. Because intense atmospheric rivers bring substantial precipitation amounts that extend far into the interior of the western U.S, we show that a network of tree-ring chronologies across this region can predict when atmospheric rivers made landfall along the coast. This enables a better understanding of past variability in these storms, which can be used to contextualize observed trends or predicted changes in storm frequency under anthropogenic climate change.

1. Introduction

Along much of the western coast of the U.S., precipitation primarily accumulates over the cold season (October-March) and is driven by synoptic-scale cyclones originating over the Pacific Ocean. Some of these cyclones are associated with atmospheric rivers (ARs), filamentary organizational processes that transport substantial amounts of moisture from the subtropical and tropical oceans towards the coastline, which then precipitates out under orographic lift along the Peninsular, Sierra Nevada, and Cascade ranges [Zhu and Newell, 1994]. ARs are a major societal

hazard in the region linked to extreme precipitation and severe flooding [Dettinger, 2004; Ralph et al., 2006]. They are also a critical source of water supply, particularly in the Mediterranean and semiarid regions of central and southern California, where they are estimated to deliver between 30-50% of the total precipitation [Guan et al., 2010; Dettinger et al., 2011; Dettinger, 2013].

While much of the moisture associated with ARs is removed on the western side of mountain ranges near the coast of western North America, these storms can deliver moisture further inland. ARs have recently been identified as an important source of water supply and a driver of extreme events during the cold season in the semiarid U.S. Intermountain West (defined as the region between the Peninsular, Sierra Nevada, and Cascade ranges on the west and Rockies on the east) [Rutz and Steenburgh, 2012]. In the Southwest, ARs that penetrate the Peninsular Range running along southern California and the Baja Peninsula have been associated with extreme floods in major watersheds like the Verde and Salt River Basins [Neiman et al., 2013; Hughes et al., 2014; Demaria et al., 2017]. Rivera et al. [2014] identified two primary storm tracks among days when ARs hit the Verde Basin: 1) a zonally oriented track that originates far to the west near Hawaii and is associated with a midlevel offshore trough west of central California and 2) a shorter, meridional track associated with a midlevel cutoff low over the Pacific off the west coast of the Baja Peninsula. Similar storm tracks were also identified by Rutz et al. [2014, 2015] and Alexander et al. [2015] as part of a larger typology of preferential pathways for ARs that penetrate into the Intermountain West. These studies showed that substantial water vapor depletion over major topographic barriers (e.g., the High Sierra) cause ARs to rapidly decay from the coastline, but conduits of milder terrain can funnel ARs further into the continental interior.

These fixed orographic conduits vary latitudinally within gaps in the Cascades, Sierra Nevada, and Peninsular Ranges and influence the proportion of ARs that penetrate into the Intermountain West and their path over land.

The tendency of ARs to penetrate into the continental interior is related to their wind speed and moisture content [Rutz et al., 2015]. Intense ARs that are more prone to cause large-scale extreme precipitation along the western U.S. coast are also likely to penetrate into the Intermountain West. In this study, we examine whether the large network of tree-ring chronologies along the US west coast and across the Intermountain West can inform us as to the frequency of incidence of ARs and associated extreme precipitation. This study builds on past work that has shown that tree-ring chronologies can be used to reconstruct the occurrence of and gradients in precipitation in the Southwest and California [Woodhouse and Meko 1997; Meko et al., 2011], as well as pressure patterns and storm tracks in the Pacific Northwest [Wise and Dannenberg, 2014, 1017]. Here we contribute a more focused examination on extreme precipitation and associated ARs. We recognize that persistent, moderate precipitation delivered from weaker extratropical cyclones can contribute substantially to seasonal rainfall, especially in years where ARs are not active, and hence extreme precipitation events are limited. However, recently we found that the potential to link extreme precipitation to a tree-ring based reconstruction of the summer Palmer Drought Severity Index (PDSI) is high in the Southwest [Steinschneider et al., 2016]. Annual tree growth increments are highly responsive to moisture from extreme winter precipitation through subsequent snowmelt during the growing season in this region [Woodhouse and Meko, 1997; Williams et al. 2010; St. George and Ault 2014], but are relatively insensitive to summer

precipitation associated with the North American Monsoon due to high rates of evaporation [St. George et al., 2010]. Therefore, we maintain a regional focus on the U.S. Southwest in this work.

We find that the two primary modes of variability in a gridded, 500-year tree-ring based reconstruction of the summer PDSI across the Southwest U.S. are associated with the two primary AR storm track patterns over the region, as identified by Rivera et al. [2014] and confirmed in later work [Rutz et al., 2014, 2015; Alexander et al., 2015; Swales et al., 2016]. We also find that the two modes of variability in tree-ring based moisture relate to the occurrence of extreme precipitation in the region, particularly in areas along the southern California coast and in southwest Arizona. We use a generalized linear regression directly on a network of chronologies sensitive to cold-season moisture across the U.S. west coast and the Intermountain West to reconstruct the variability of AR landfalls along the southern California coastline, as well as extreme precipitation occurrences and amounts on the west coast near Los Angeles. The reconstructions accurately reproduce the variability in AR landfalls and extreme precipitation occurrences during the instrumental record, with significant but weaker regression results on the average magnitude of extreme precipitation amounts. The reconstructions also align well with documented extreme events in the 19th century. To our knowledge, this is the first attempt to reconstruct the occurrence of storm tracks and associated extreme precipitation events in the Southwest US based on a network of tree-ring chronologies.

2. Relating rotated EOFs of tree-ring based moisture to Southwest ARs

The first part of the analysis is based on the Living Blended Drought Atlas (LBDA) [Cook et al., 2010], which is the latest update of the North American Drought Atlas [Cook et al., 1999] and provides a reconstruction of the summer PDSI from 1451-2005 based on a point-by-point regression with tree-ring chronologies within a 450 km search radius. We perform an Empirical Orthogonal Function (EOF) analysis on the LBDA over the entire record across the west coast and Intermountain West in a region west of 105°W between 23°N and 40°N (hereafter referred to as the Southwest LBDA), and retain the first two EOFs (containing ~80% of the total variability) before applying a varimax rotation (Figure 1a,b). Within the defined region, the LBDA has been shown to relate strongly to winter precipitation, but has no significant relationship to summertime precipitation, allowing the winter signal to be isolated [St. George et al., 2010]. The leading rotated component (RPC1) represents a north-south oriented footprint of moisture extending from central Mexico to southern Wyoming with a center located between southern Arizona and New Mexico. The second mode (RPC2) maintains a southwest-to-northeast orientation that extends from southwestern California to the western edge of the Rocky Mountains, with a primary lobe centered in southern California and Nevada. These spatial patterns are very consistent if the rotated EOF analysis is conducted over different 100-year periods of record, although the two modes can switch order (see Figure S1).

We correlate average cold-season (October-March) 500 hPa geopotential heights between 1949-2005 from the NCEP/NCAR Reanalysis I (2.5° by 2.5°; Kalnay et al., [1996]) to the RPCs associated with the first two modes of the Southwest LBDA, and composite anomalous, cold-season integrated water vapor transport (IVT) from the same reanalysis dataset for the years with

the 20 largest values for each RPC. The first mode of the Southwest LBDA is related to a confined low-pressure center over Northwestern Mexico that drives a strong meridional IVT from the eastern subtropical Pacific through western Mexico and into the Southwest US. This pattern resembles the second mode of IVT variability identified by Rivera et al. [2014], although the associated midlevel cutoff low and IVT is located further east over the Southwest. The second mode of the Southwest LBDA is associated with a broader trough off the California coast that drives a longer and zonally oriented flux of IVT from the central subtropical Pacific towards the southern California coastline. This pattern resembles the first mode of IVT variability identified by Rivera et al. [2014], although the trough and IVT is shifted further to the north. The differences from the results in Rivera et al. [2014] reflect the regional scale of our analysis and are similar to AR pathways identified in Rutz et al. [2015] (their Figure 16), and suggest that the first two leading modes of variability in the Southwest LBDA record major modes of IVT variability that represent key AR typologies impacting the Southwest.

The relationships in Figure 1 suggest that the leading modes of Southwest LBDA variability may also record information regarding the risk of extreme precipitation in the Southwest associated with landfalling ARs. Using the daily, gridded precipitation dataset of Livneh et al. [2013], we calculate the number and average magnitude of extreme precipitation events in the cold season for each year, defined as any precipitation event that exceeds the 99.5th percentile (approximately two events per year on average). We correlate the occurrence and magnitude of extreme precipitation with both RPC1 and RPC2 of the Southwest LBDA (Figure 2). We find that RPC1 informs both the occurrence and average magnitude of extreme precipitation in a region centered

in southwestern Arizona, while RPC2 is more strongly related to the occurrence and to a lesser extent the magnitude of extreme precipitation in southern California. Both patterns are consistent with the storm track orientations in Figure 1. Spearman correlation values upwards of 0.6-0.65 are noted in certain regions of California and Arizona. Consistent with the results of Woodhouse and Meko [1997], the relationship is stronger with extreme precipitation occurrence than average magnitude, since the tree-ring based moisture proxy is likely more sensitive to the total precipitation delivered (which is well represented by the number of extremes) rather than resolving the average degree of wetness for any event.

Overall, the relationships in Figure 2 suggest the potential to reconstruct the risk of extreme precipitation occurrences and to a lesser degree its magnitude based on spatial patterns in the LBDA. However, even in the regions with strongest correlations, there are times when the RPCs are elevated but few if any extremes occurred (not shown), suggesting that the modes of the Southwest LBDA in these cases are being driven by less extreme precipitation. We explored how varying the threshold of extreme precipitation through the set of 85th, 90th, 95th, and 99th percentile of daily precipitation values changes the correlation maps in Figure 2 (Figure S2). These maps show that an increasing amount of the variability in the occurrence of extreme precipitation can be explained by RPC1 and RPC2 as the threshold used to define extreme precipitation is relaxed, with Spearman correlation coefficients upwards of 0.75 across a broad swath of the Southwest if the threshold is decreased to the 95th percentile (approximately 18 events per year). The variance explained ceases to change much once the threshold is reduced to between the 85th and 90th percentile, which coincides with precipitation amounts near zero in the Southwest (i.e., total cold-

season precipitation). Importantly though, the amount of variability explained for the average magnitude of extremes does not noticeably improve as the threshold is relaxed, again indicating that the tree-ring based proxies may be better suited to identify the occurrence of extreme precipitation in the region.

3. Reconstruction of ARs and extreme rainfall in southern California

The composites of IVT in Figure 1 and the relationships to extreme precipitation in Figure 2 suggest that information recorded by dendroclimatic proxies in southern California and extending towards the Rockies in Colorado is related to the landfall of ARs along the southwest coastline. Further, tree-ring chronologies in Mexico and southern Arizona and New Mexico may be inversely related to the occurrence of ARs impacting the southern California coast, as the occurrence of the cutoff low associated with RPC1 may reduce the likelihood of the midlevel trough off the California coast associated with RPC2 in the same season. To explore the potential to reconstruct AR variability based on these findings, we collect occurrences of AR landfalls along the southern California coast (south of 38°N, see Figure 1) from the recent dataset of Brands et al. [2017]. ARs in this dataset are defined based on IVT calculated over different periods from four reanalysis products: NCEP/NCAR Reanalysis 1 (NCEP/NCAR, Kalnay et al., [1996]), NOAA CIRES twentieth-century reanalysis v2 (NOAA-20C, Compo et al. [2011]), ECMWF ERA-20C reanalysis (ERA-20C, Poli et al. [2013]), and ECMWF ERA-interim reanalysis (ERA-Interim, Dee et al. [2011]). The dataset provides different AR landfall occurrences for different combinations of AR detection and tracking thresholds, enabling a sensitivity analysis based on the definition of ARs (see Supporting Information for more detail).

For the three longer reanalysis products (NCEP/NCAR, NOAA-20C, ERA-20C), we produce an annual time series of the frequency of ARs impacting the southern California coast each cold-season for 1950-1990. We then conduct a Poisson regression to relate the occurrence of landfalling ARs directly to a network of chronologies that are sensitive to cold-season moisture across the U.S. west coast and the Intermountain West. These chronologies, which most often extend to 1990, have been pre-screened from the larger regional network to ensure that they only record significant variations in cold-season precipitation [Torbenson, 2018]. A lasso penalty is applied in the regression for simultaneous model selection and fitting. Model fitting, evaluation, and uncertainty estimation is described in the Supporting Information. The final reconstruction of AR occurrences uses a nested set of three separate regressions based on different sets of chronologies due to the difference in chronology length over the 1451-1990 time period.

Figure 3a shows the rank correlation between each chronology and the number of AR landfall occurrences from the ERA-20C reanalysis. Other reanalysis products yielded similar results (Figure S3). As expected, many of the chronologies in southern and central California are well correlated with AR landfalls. However, similar to the pattern of RPC2 in Figure 1, there are also significant relationships with chronologies further into the Intermountain West, including in northwestern Arizona and western New Mexico and Colorado, indicating that the penetration of these ARs into the Intermountain West leaves a footprint of moisture along their path into the continental interior. AR landfalls are also significantly and inversely correlated to some chronologies in central Mexico, suggesting that rainfall in that region becomes less likely as the number of AR landfalls increase along the southwest California coastline. This could be because

a persistent trough to the west of central California associated with a high number of AR landfalls along the coastline reduces the likelihood of a strong cutoff low over the Baja Peninsula linked to the meridional ARs associated with RPC1 in Figure 1. Chronologies in all of the regions mentioned above were selected by the final set of nested regressions (Figure S4), which fit the observed number of AR landfall occurrences during the instrumental period very well (Figure 3b) and provide between a 63-74% improvement over a stationary Poisson model (as determined by its deviance ratio, see Supporting Information for more detail). The reconstruction of AR landfalls (Figure 3c) also shows large increases during times of well-documented floods in southern and central California and parts of Arizona prior to the instrumental record used here (i.e., prior to 1950), including the Great Flood of 1862 and extending through a series of floods in southern California and Arizona in the late 19th and early 20th centuries (e.g., 1868, 1890, 1891, 1906, 1907, 1909, 1916, 1941) [Dobyns, 1981; Paulson et al., 1989]. The reconstruction also shows a notable decrease in AR landfalls in the second half of the 1400's and first half of the 1500's, which has been associated with increased drought activity in the Southwest [Cook et al., 2014], although a large peak in AR landfalls punctuates this period in the late 1400's. We note that the linear relationship found between AR landfall occurrences and chronologies, even during the largest flood events in the historical record, is likely associated with additional chronologies recording a strong moisture signal over a wider region, since tree growth at any one location may not respond beyond some upper threshold of available moisture. Finally, we also examine the sensitivity of the above model to the definition of ARs based on different detection and tracking algorithms used in the Brands et al. [2017] dataset. We find that lower IVT thresholds, particularly for AR detection, generally improve the relationship with AR landfall occurrences

(Figure S5). This is consistent with the results in Figure S2 and suggests that the tree-ring chronologies are better able to reconstruct the risk of all large storms, not just the most extreme.

The AR landfalls used above extend across a long stretch of California coastline and therefore could impact extreme precipitation and flooding in multiple areas, including central and southern California and parts of Arizona and New Mexico (see AR pathways in Rutz et al., [2015], their Figure 16). To create a more locally focused reconstruction of extremes, we perform a similar Poisson lasso regression against the occurrence of extreme precipitation events in Los Angeles based on the long precipitation record at the Los Angeles airport. We also perform a linear regression against the logarithm of the non-zero average magnitude of exceedances.

Similar to AR landfalls, the nested regression models for extreme precipitation occurrences also select chronologies in the Intermountain West for the final reconstruction (Figure S6). Again, this is consistent with the AR tracks associated with RPC2 that impact southern California and travel south of the High Sierra before extending further inland into southern Nevada and Utah. The nested regressions accurately explain the variability in the observed data (Figure 4a, also see Figure S7a), providing between a 50-60% improvement over a stationary Poisson model, and align well with historic records of past flood years in southern California (Figure 4c, Paulson et al., [1989]). We note though that the reduction in variance of extreme precipitation occurrences prior to 1600 is an artifact of fewer available chronologies in that period. Thus, the magnitude of the reconstruction across time periods should be compared separately for each of the three nested regression models (see Figure S8).

The regression on extreme precipitation amounts is much less accurate than that for occurrences (Figure 4b, also see Figure S7b). Accordingly, we omit presenting the reconstruction of extreme precipitation amounts. The lack of skill again confirms that the tree-ring chronologies are likely better suited to record the occurrence of wet conditions than the average magnitude of extreme precipitation across events. Importantly, however, ARs tend to leave specific spatial signatures of moisture distributed across the coast and Intermountain West and the spatial patterns among growth anomalies in a large network of tree-ring chronologies shows great promise for being able to reconstruct these extreme events.

4. Conclusion

This work showed for the first time that a network of tree-ring chronologies across the west coast of the U.S. and the Intermountain West can be used to reconstruct the occurrence of AR storm tracks and associated extreme precipitation in that region. In the Southwest, these chronologies record the footprint of cold-season moisture associated with the two primary AR storm tracks that influence the region as they pass through the Peninsular and Sierra Nevada ranges into the interior of the U.S. along preferred, filamentary pathways. The Southwest U.S. focus was motivated by the availability of a gridded, tree-ring based moisture product that is able to isolate cold-season precipitation in that region. Future work will attempt to extend the reconstruction of AR landfalls and extreme precipitation to other regions along the North American west coast, such as the U.S. Pacific Northwest. In that region, conduits of low elevation in the Cascades steer ARs deep into the Intermountain West through eastern Oregon and along the Snake River plain

into the northern Rocky Mountains of central Idaho and western Montana [Rutz et al., 2014, 2015; Alexander et al., 2015]. Tree-ring chronologies along this path, particularly at the terminus in Idaho and Montana, could be used to reconstruct occurrences of this northern AR trajectory. Recent efforts towards this end have shown promise [Wise and Dannenberg, 2017]. However, larger summer precipitation totals and lower evaporation rates in the Pacific Northwest will require additional care in isolating the wintertime signal, which is becoming increasingly possible by using earlywood and latewood chronologies [Crawford et al., 2015].

If AR landfall occurrences and associated extreme precipitation for different latitudinal bands of western North America can be successfully reconstructed from the network of tree-ring chronologies across the coast and Intermountain West, then the potential exists to combine these reconstructions into an integrated framework to reconstruct long-term, structured fluctuations in the latitudinal variability of AR activity. The goal would be to infer slowly varying shifts in the organization of atmospheric circulation that steer ARs towards the west coast, which manifest in the frequency and magnitude of regional extreme precipitation that is recorded by the chronologies across the coast and Intermountain West in preferred spatial patterns. There could be a mixture of AR landfalls across different latitudinal bands in any given year, but it is likely that the large-scale circulation leads to a preferred subset of storm patterns with similar orientation contributing to extremes in a given year. The organization in this process could be explored formally using a latent variable model as a unifying statistical framework, where slowly varying components of the climate system could be modeled as a latent (i.e., unobservable) process with smooth fluctuations that can be inferred from noisier fluctuations in modes of

extreme precipitation, cold-season chronologies, and AR occurrences. The latent process can be extended backward in time based on the long tree-ring based field, and can then be subsequently used to reconstruct extreme regional precipitation risk and AR landfall occurrences with the appropriate degree of uncertainty. This effort is left for future work.

Acknowledgements

Much of the data used in this analysis is publicly available through NOAA online repositories, including the gridded precipitation, NCEP reanalysis, and LBDA. We thank Dave Stahle, Dorian Burnette, Daniel Griffin, and Max Torbenson for providing the cold-season precipitation-sensitive tree-ring chronologies used here, which are available from the International Tree-Ring Data Bank at NOAA (<http://www.ncdc.noaa.gov/data-access/paleoclimatology-data/datasets/tree-ring>). We also thank Swen Brands for providing the database of landfalling atmospheric rivers, which is available at <http://www.meteo.unican.es/atmospheric-rivers>. The authors acknowledge support from NOAA and from NSF Grants AGS1702273, AGS1702184, AGS1703029, and AGS1301587. Lamont-Doherty Earth Observatory contribution number xxxx.

References

Alexander, M.A., Scott, J.D., Swales, D., Hughes, M., Mahoney, K., and Smith, C.A., (2015), Moisture pathways into the U.S. Intermountain West associated with heavy winter precipitation events, *Journal of Hydrometeorology*, 16, 1184-1206.

- Brands, S., Gutiérrez, and San-Martín, D. (2017), Twentieth-century atmospheric river activity along the west coasts of Europe and North America: algorithm formulation, reanalysis uncertainty and links to atmospheric circulation patterns, *Climate Dynamics*, 48, 2771-2795, doi: 10.1007/s00382-016-3095-6.
- Compo GP, Whitaker JS, Sardeshmukh PD, Matsui N, Allan RJ, Yin X, Gleason BE Jr, Vose RS, Rutledge G, Bessemoulin P, Broen- nimann S, Brunet M, Crouthamel RI, Grant AN, Groisman PY, Jones PD, Kruk MC, Kruger AC, Marshall GJ, Maugeri M, Mok HY, Nordli O, Ross TF, Trigo RM, Wang XL, Woodruff SD, Worley SJ (2011), The twentieth century reanalysis project. *Q J R Meteorol Soc* 137(654, A):1–28. doi:10.1002/qj.776
- Cook, B.I., Smerdon, J.E., Seager, R., and Cook, E.R. (2014), Pan-continental droughts in North America over the last millennium, *27* (1), 383-397.
- Cook, E.R., Meko, D.M., Stahle, D.W., and Cleaveland, M.K. (1999), Drought reconstructions for the continental United States, *Journal of Climate*, 12(4), 1145-1163.
- Cook, E.R., Seager, R., Heim, R.R., Vose, R.S., Herweijer, C., and Woodhouse, C. (2010), Megadroughts in North America: Placing IPCC projections of hydroclimatic change in a long-term paleoclimate context. *Journal of Quaternary Science*, 25(1), 48-61. doi: 10.1002/jqs.1303

Crawford, C. J., D. Griffin, and K. F. Kipfmueller (2015), Capturing season- specific precipitation signals in the northern Rocky Mountains, USA, using earlywood and latewood tree rings, *J. Geophys. Res. Biogeosci.*, 120, 428–440, doi:10.1002/2014JG002740

Dee DP, Uppala SM, Simmons AJ, Berrisford P, Poli P, Kobayashi S, Andrae U, Balmaseda MA, Balsamo G, Bauer P, Bechtold P, Beljaars ACM, van de Berg L, Bidlot J, Bormann N, Delsol C, Dragani R, Fuentes M, Geer AJ, Haimberger L, Healy SB, Hersbach H, Holm EV, Isaksen L, Kallberg P, Koehler M, Matri- cardi M, McNally AP, Monge-Sanz BM, Morcrette JJ, Park BK, Peubey C, de Rosnay P, Tavolato C, Thepaut JN, Vitart F (2011) The ERA-interim reanalysis: configuration and performance of the data assimilation system. *Q J R Meteorol Soc* 137(656, Part a):553–597. doi:10.1002/qj.828

Demaria, E. M. C., Dominguez, F., Hu, H., von Glinski, G., Robles, M., Skindlov, J., and Walter, J. (2017), Observed hydrologic impacts of landfalling atmospheric rivers in the Salt and Verde river basins of Arizona, United States. *Water Resources Research*, 53. <https://doi.org/10.1002/2017WR020778>

Dettinger, M.D. (2004), Fifty-Two Years of Pineapple-Express Storms Across the West Coast of North America. California Energy Commission PIER Energy-Related Environmental Research Report CEC-500-2005-004, Sacramento, California, 15 pp.

Dettinger, M.D. (2013), Atmospheric rivers as drought busters on the U.S. west coast, *Journal of Hydrometeorology*, 14(5), 1721-1732.

Dettinger, M.D., Ralph, F.M., Das, T., Neiman, P.J., Cayan, D.R. (2011), Atmospheric rivers, floods, and the water resources of California. *Water*, 2011(3), 445–478. DOI: 10.3390/w3020445.

Dobyns, H.R. (1981), *From fire to flood, Historic human destruction of Sonoran desert riverine oases: Socorro, New Mexico*, Ballena Press, 222 p.

Guan, B., Molotch, N. P., Waliser, D. E., Fetzer, E. J., and Neiman, P. J. (2010), Extreme snowfall events linked to atmospheric rivers and surface air temperature via satellite measurements, *Geophys.Res. Lett.*, 37, L20401, doi:10.1029/ 2010GL044696.

Hughes, M., Mahoney K.M., Neiman, P.J, Moore, B.J., Alexander, M., and Ralph, F. M. (2014), The landfall and inland penetration of a flood-producing atmospheric river in Arizona. Part II: Sensitivity of modeled precipitation to terrain height and atmospheric river orientation, *Journal of Hydrometeorology*, 15 (5), 1954-1974.

Kalnay, E., M. Kanamitsu, R. Kistler, W. Collins, D. Deaven, L. Gandin, M. Iredell, S. Saha, G. White, J. Woollen, Y. Zhu, A. Leetmaa, R. Reynolds, M. Chelliah, W. Ebisuzaki, **W.**

- Higgins, J. Janowiak, K. C. Mo, C. Ropelewski, J. Wang, R. Jenne, D. Joseph, A. Leetmaa, R. Reynolds, R. Jenne, and D. Joseph (1996), The NCEP/NCAR 40-Year Reanalysis Project, *Bulletin of the American Meteorological Society*, 77(3), 437–471, doi: 10.1175/1520-0477(1996)077<0437:TNYRP>2.0.CO;2.
- Livneh B., E.A. Rosenberg, C. Lin, B. Nijssen, V. Mishra, K.M. Andreadis, E.P. Maurer, and D.P. Lettenmaier (2013), A Long-Term Hydrologically Based Dataset of Land Surface Fluxes and States for the Conterminous United States: Update and Extensions, *Journal of Climate*, 26, 9384–9392.
- Meko, D.M., Stahle, D.W., Griffin, D., and Knight, T.A. (2011), Inferring precipitation-anomaly gradients from tree-rings, *Quaternary International*, 235 (1-2), 89-100.
- Neiman, P.J., Ralph, F. M., Moore, B.J., Hughes, M., Mahoney, K.M., Cordeira, J.M., and Dettinger, M.D. (2013), The landfall and inland penetration of a flood-producing atmospheric river in Arizona. Part I: Observed synoptic-scale, orographic, and hydrometeorological characteristics, *Journal of Hydrometeorology*, 14, 460-484.
- Paulson, R.W., Chase, E.B., Roberts, R.S., and Moody, D.W., Compilers, National Water Summary 1988-89-- Hydrologic Events and Floods and Droughts: U.S. Geological Survey Water-Supply Paper 2375, 591 p.

Poli P, Hersbach H, Tan D, Dee D, Thépaut JN, Simmons A, Peubey C, Laloyaux P, Komori T, Berrisford P, Dragani R, Trémolet Y, Hólm E, Bonavita M, Isaksen L, Fisher M (2013), The data assimilation system and initial performance evaluation of the ECMWF pilot reanalysis of the 20th-century assimilating surface observations only (era-20c). Technical report, ERA report series 14

Ralph, F. M., P. J. Neiman, G. A. Wick, S. I. Gutman, M. D. Dettinger, D. R. Cayan, and A. B. White (2006), Flooding on California's Russian River: Role of atmospheric rivers, *Geophys. Res. Lett.*, 33, L13801, doi:10.1029/2006GL026689.

Rivera, E.R., Dominguez, F., and Castro, C.L. (2014), Atmospheric rivers and cool season extreme precipitation events in the Verde River Basin of Arizona, *Journal of Hydrometeorology*, 15 (2), 813-829.

Rutz, J.J., and Steenburgh W.J. (2012), Quantifying the role of atmospheric rivers in the interior western United States, *Atmospheric Science Letters*, 13, 257-261.

Rutz, J.J., Steenburgh W.J., and Ralph, F.M. (2014), Climatological characteristics of atmospheric rivers and their inland penetration over the Western United States, *Monthly Weather Review*, 142, 905-921.

- Rutz, J.J., Steenburgh W.J., and Ralph, F.M. (2015), The inland penetration of atmospheric rivers over Western North America: a Lagrangian analysis, *Monthly Weather Review*, 143, 1924-1944.
- St. George, S., Ault, T. R. (2014), The imprint of climate within Northern Hemisphere trees, *Quaternary Science Reviews*, 89, 1-4, doi:10.1016/j.quascirev.2014.04.029.
- St. George, S., Meko, D.M., and Cook, E.R. (2010), The seasonality of precipitation signals embedded within the North American Drought Atlas, *Holocene*, 20(6), 983-988.
- Swales, D., M. Alexander, and M. Hughes (2016), Examining moisture pathways and extreme precipitation in the U.S. Intermountain West using self-organizing maps, *Geophys. Res. Lett.*, 43, 1727–1735, doi:10.1002/2015GL067478.
- Torbenson, M.C.A. (2018), Cool and warm season climate signals in tree rings from the Americas. PhD Dissertation, Dept. of Geosciences, University of Arkansas, Fayetteville, 180 pp.
- Williams, A. P., J. Michaelsen, S. W. Leavitt, and C. J. Still (2010), Using tree-rings to predict the response of tree growth to climate change in the continental United States during the 21st century, *Earth Interactions*, 14(19), 1-20, doi:10.1175/2010EI362.1.

Wise, E.K., and Dannenberg, M.P. (2014), Persistence of pressure patterns over North America and the North Pacific since AD 1500, *Nature Communications*, 5, 4912, doi:10.1038/ncomms5912.

Wise, E.K., and Dannenberg, M.P. (2017), Reconstructed storm tracks reveal three centuries of changing moisture delivery to North America, *Science Advances*, 3(6), e1602263, doi:10.1126/sciadv.1602263.

Woodhouse, C.A., and Meko, D.M. (1997), Number of winter precipitation days reconstructed from Southwestern Tree Rings, *Journal of Climate*, 10, 2663-2669.

Zhu, Y., and R. E. Newell (1994), Atmospheric rivers and bombs, *Geophys. Res. Lett.*, 21, 1999–2002, doi:[10.1029/94GL01710](https://doi.org/10.1029/94GL01710).

Figure Captions

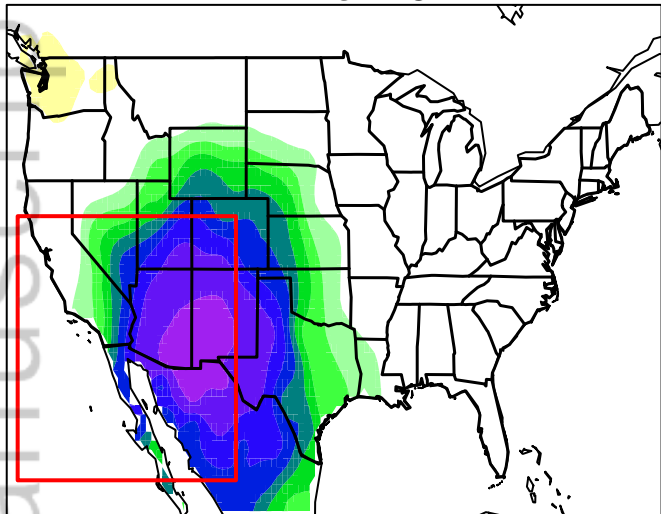
Figure 1. Spearman correlation between the RPCs of the first 2 rotated EOFs of the Southwest LBDA (boxed region) and (top) the gridded LBDA across North America and (bottom) Oct.-Mar. average 500 hPa geopotential height anomalies. Composites of anomalous Oct.-Mar. integrated water vapor transport (IVT) for the years with the 20 largest RPC values are shown as arrows in the bottom figures (maximum IVT shown is $285 \text{ kg m}^{-1}\text{s}^{-1}$). A transect for counts of landfalling ARs is shown in blue.

Figure 2. Spearman correlations between the occurrence (top) and average magnitude (bottom) of extreme daily precipitation events during the cold season (Oct.-Mar.) with RPC1 (left) and RPC2 (right) of the Southwest LBDA between 1949-2005. Correlation values near Los Angeles are highlighted.

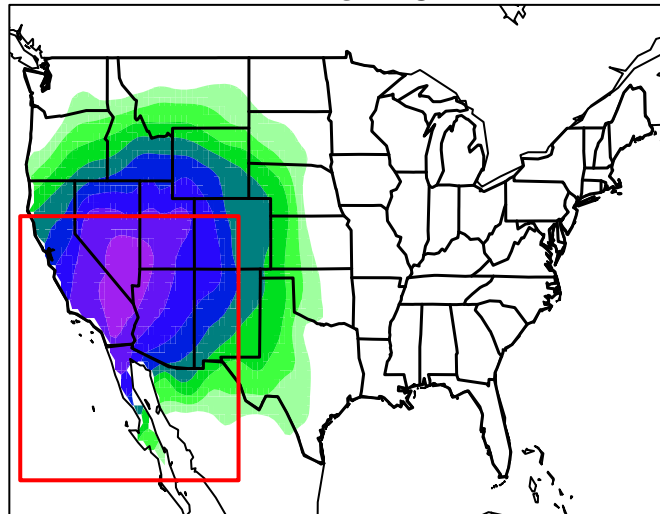
Figure 3. a) Spearman correlation between number of landfalling ARs along the southern coast of California and cold-season chronologies between 1950-1990 b) Observed versus predicted number of landfalling ARs from 1950-1990 based on a Poisson regression using a lasso penalty and 102 available chronologies c) Time series of observed (red) and reconstructed (black) AR landfall occurrences using a Poisson lasso regression, with 95% prediction interval.

Figure 4. Observed versus predicted (a) number of extreme precipitation occurrences and b) extreme precipitation amounts in Los Angeles between 1950-1990, based on a Poisson regression and linear regression on log transformed non-zero values, respectively. c) Time series of observed and reconstructed precipitation occurrences with 95% predictive interval.

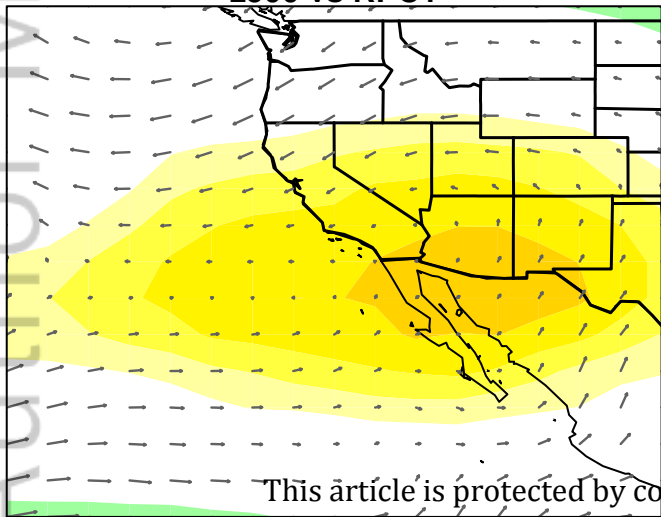
LBDA vs RPC1



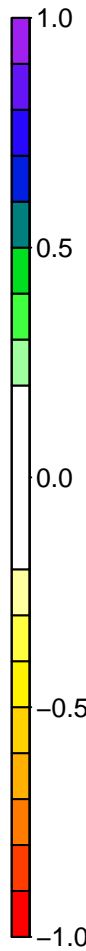
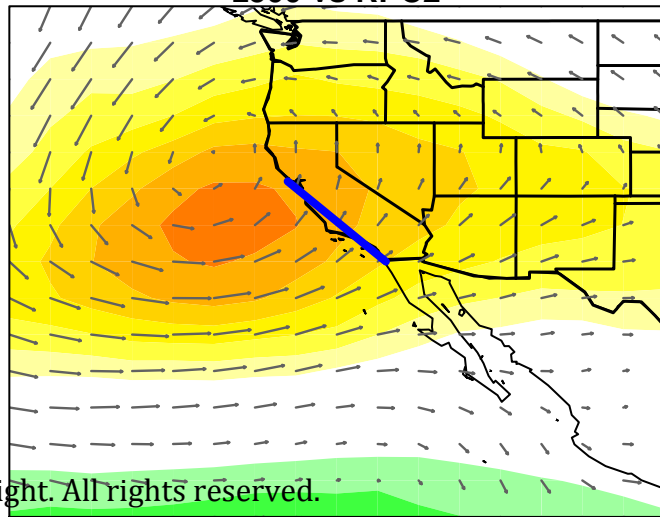
LBDA vs RPC2



z500 vs RPC1



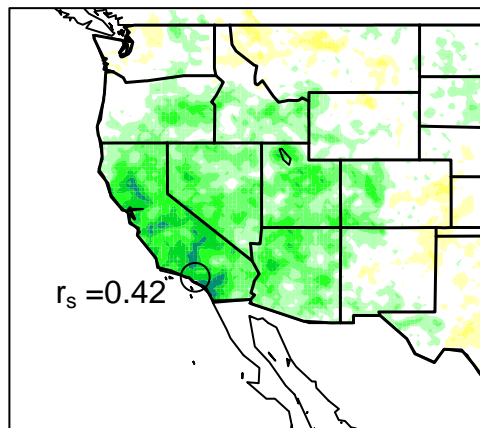
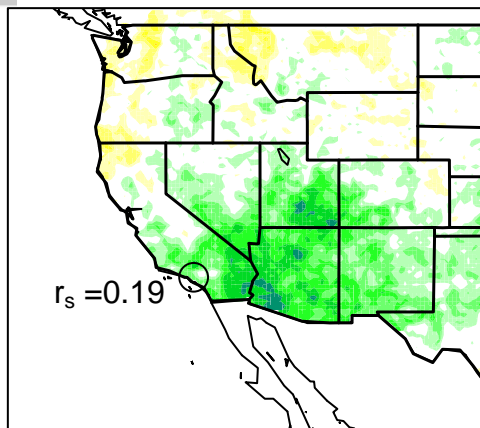
z500 vs RPC2



RPC1 correlation

RPC2 correlation

exceedance (99.5%):
occurrence



exceedance (99.5%):
mean amount

